Supporting Information for

Enabling Natural Abundance ^{17}O Solid State NMR by Direct Polarization from Paramagnetic Metal Ions

Daniel Jardón-Álvarez(1), Guy Reuveni(1), Adi Harchol(1), Michal Leskes*(1)

(1) Department of Materials and Interfaces, Weizmann Institute of Science, Rehovot, 76100, Israel

1. Line shape analysis

The measured ^{17}O DNP MAS spectra presented three sharp peaks (FWHM ~ 50 ppm) at 536, 441 and 380 ppm, with large spinning sideband manifolds, attributed to first order quadrupolar broadening, on top of a very broad component (FWHM > 1000 ppm). This broad component is not visible with direct excitation[1], but requires a Hahn echo experiment. Figure S1 a) shows a small increment in the relative intensity of the broad peak, when increasing the Fe(III) content from x=0.00125 to 0.02. Most surprisingly, broad and sharp signals do not show any significant difference in longitudinal magnetization build-up times (see Figure S1 b)).

The much smaller quadrupolar coupling constant of ^{6}Li compared to ^{17}O enables an in-depth study of the effect of paramagnetic centers on its NMR line shape. First, we notice that none of the samples presented an extremely broad peak, as observed on ^{17}O, this was

further confirmed by observing no significant difference between direct excitation and Hahn echo measurements (not shown here). Further, the ^{6}Li line shape cannot be deconvoluted satisfactory with a single Lorentzian or Gaussian shaped function. Reasonable agreements can be obtained using two Lorentzian lines, however, the properties of these lines are not conserved when modifying concentration or recycle delay of the measurement (see Figure S2 c)). Instead we attribute the line shape to a distribution of Lorentzian peaks, whose broadening reflects the distance to the nearest paramagnetic dopant. Note that this "stretched Lorentzian" (broader on the base and sharper in the center compared to a regular Lorentzian) is the result of the Fourier transform of a stretched exponential decay in the time domain.

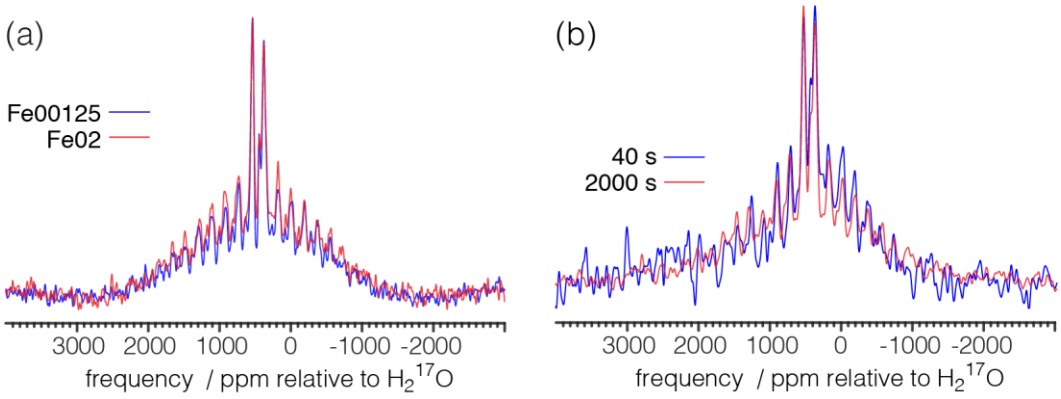

Figure S1. ^{17}O DNP MAS Hahn echo spectra a) after full recovery in Fe00125LTO and Fe02LTO and b) after 40 and 2000 s build-up time in Fe005LTO.

The trends observed on evolution of the full width at half maximum (FWHM) shown in Figure S2 a) and b) are in agreement with a model of a distribution of relaxation times and line broadenings due to the distribution of distances to the paramagnetic center. An overall

broadening is observed with increasing Fe(III) content, as the average distance between paramagnetic sites becomes shorter. The FWHM becomes smaller with increasing build-up times, as nuclei in proximity to paramagnetic center are not only broadened but also have shorter $T_{1,BU}$. Most remarkably, the linewidth obtained after full recovery with and without µW irradiation are indistinguishable within the error, indicating that hyperpolarization has spread through the entire sample.

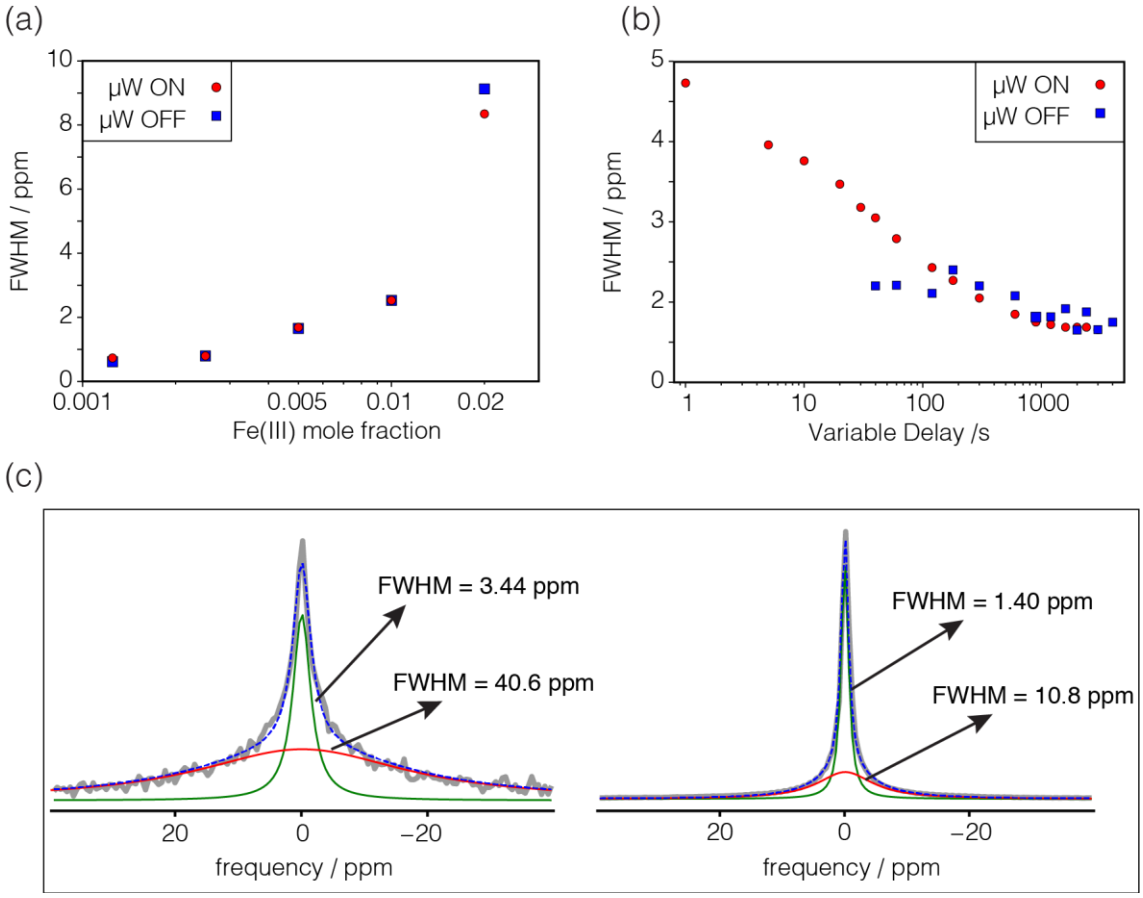

Figure S2. Full width at half maximum (FWHM) of ^{6}Li spectra a) with varying concentration and after full magnetization build-up (>90% magnetization) and b) at fixed Fe(III) content of $x = 0.005$ (Fe005LTO) and variable magnetization build-up time. c) Best line shape deconvolution of the ^{6}Li DNP MAS signal in Fe005LTO using two Lorentzian functions after a recycle delay of 1 (left) and 3000 s (right).

2. Relaxation

As we have mentioned previously, fitting of the saturation recovery spectra via deconvolution of the spectrum with two Lorentzian functions does not give any meaningful result, as a consequence of the changes in the line shape. It is possible, nonetheless, to fit the evolution of the integrated area using two exponential functions:

$$M_z(t) = A \cdot \left[1 - \exp\left[-\left(t/T_{1,BU(A)}\right)\right]\right] + B \cdot \left[1 - \exp\left[-\left(t/T_{1,BU(B)}\right)\right]\right]. \quad \text{(S1)}$$

Where the fast relaxing component might be attributed to core nuclei, in close proximity to the paramagnetic center, and the slow relaxing to the bulk in which all nuclei have a common spin temperature due to spin diffusion. Results are given in Table S1. In general we observe a reasonable agreement between T_1 (relaxation without μW) and T_{BU} (polarization build-up time under μW irradiation). With increasing concentration, the fast relaxing component becomes more prominent, which would be in agreement with an increment in relative amount of core nuclei. However, this concept does not explain the significant reduction of $T_{1,BU}$ of the fast relaxing nuclei with concentration.

$x_{Fe(III)}$	μW	$T_{1,BU(A)}$ (s)	$T_{1,BU(B)}$ (s)	A/B
0.02	ON	22±2	3.1±0.5	0.92/1
	OFF	34±50	6±7	0.63/1
0.01	ON	180±15	23±3	1.37/1
	OFF	352±100	52±10	0.98/1
0.005	ON	371±30	34±3	1.43/1
	OFF	299±30	10±8	7.25/1
0.0025	ON	3814±170	954±100	3.78/1
	OFF	4012±440	302±70	4.17/1
0.00125	ON	4383±190	206±30	3.98/1
	OFF	4435±400	234 ±80	5.01/1

Table S1. ^{6}Li T_1 and T_{BU} obtained from fitting the integrated intensity of the saturation recovery experiments using two exponentials according to equation (S1), where $x_{Fe(III)}$ is the mole fraction of Fe(III).

A distribution of relaxation times is expected if the bulk nuclei do not have a common spin temperature. The magnetization build-up of such a system follows a stretched exponential behavior[2]. Best fits of the relaxation data obtained using equation (9) of the main document are given in Table S2. Within error margins, we have found no significant difference between T_1 and T_{BU}. Figure S3 shows the magnetization build-up times as a function of the Fe(III) concentration. The data shows a nearly inverse squared dependence with concentration, which following the discussion given in the main document is an indication of the absence of spin diffusion. In summary, we have found that the data can be explained fully with the concept of a distribution of relaxation times due to direct dipolar coupling to the dilute paramagnetic center.

$x_{Fe(III)}$	µW	$T_{1,BU}$ (s)	β	$T_{95\%}$ (s)
0.02	ON	8.6±0.3	0.61±0.02	52±4
	OFF	13±3	0.75±0.2	56±25
0.01	ON	88±3	0.68±0.01	442±20
	OFF	140±10	0.78±0.06	576±80
0.005	ON	176±5	0.63±0.01	1007±40
	OFF	272±30	0.71±0.05	1263±170
0.0025	ON	3040±60	0.87±0.01	10673±260
	OFF	3640±300	0.70±0.02	17637±1700
0.00125	ON	3920±100	0.64±0.01	21853±800
	OFF	4170±500	0.70±0.03	20447±2800

Table S2. ^{6}Li T_1 and T_{BU} obtained from fitting the integrated intensity of the saturation recovery experiments using a single stretched exponential according to equation (9) of the main document, where $x_{Fe(III)}$ is the mole fraction of Fe(III).

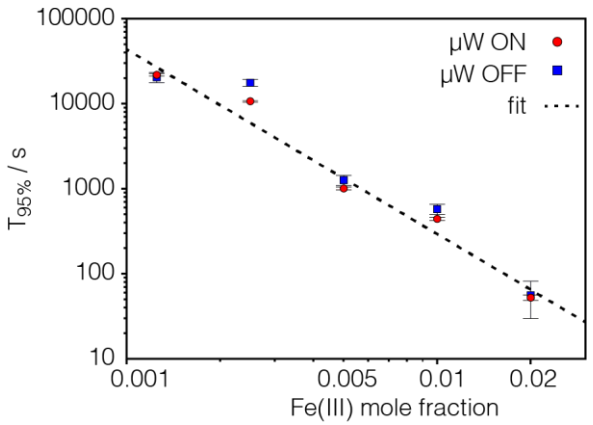

Figure S3. Build-up time of 95% of the ^{6}Li polarization obtained from fits of saturation recovery measurements with (red) and without (blue) µW irradiation. The dashed line is best fit of the µW ON data to the equation: $T_{95\%}=ac^{-b}$, with c being the Fe(III) mole fraction. Best fit parameters: a = 292 ± 100 s, b = 2.17 ± 0.25.

3. Enhancements

Table S3 andTable **S4** summarize experimental parameters, obtained signal intensities and calculated enhancements for the ^{6}Li and ^{17}O measurements.

$x_{Fe(III)}$	µW	Mass (mg)	t_1 (s)	signal recovered	ns	t_{tot} (min)	S (a.u.)	S_{norm} /scan (a.u.)	Quench factor	$\varepsilon_{ON/OFF}$	S/N	$[S/N]_{norm}$ /scan
0.02	ON	35.8	220	0.999	2	7.33	48.2	21.6	-	44±2	99	62.72
	OFF		620	1	8	82.67	4.37	0.489	0.58±0.03		6	1.90
0.01	ON	35.7	800	0.989	1	13.33	82.2	74.3	-	118±7	875	789.62
	OFF		800	0.979	1	13.33	0.693	0.63	0.76±0.04		9	8.20
0.005	ON	35.8	1650	0.983	1	27.5	102	92.6	-	142±5	1990	1811.85
	OFF		1650	0.973	1	27.5	0.71	0.65	0.78±0.04		14.5	13.34
0.0025	ON	35.5	11000	0.954	1	183.33	142	133	-	149±5	7859	7311.18
	OFF		11000	0.884	1	183.33	0.886	0.890	1.06±0.05		47	47.19
0.00125	ON	35.4	22000	0.95	1	366.67	131	122	-	146±7	6311	5879.19
	OFF		22000	0.957	1	366.67	0.904	0.836	1.00±0.05		42	38.84

Table S3. ^{6}Li parameter for the DNP measurements, where $x_{Fe(III)}$ is the mole fraction of Fe(III), t_1 the recycle delay, ns the number of scans, t_{tot} the total experimental time, S the total integrated intensity of the spectrum, S_{norm}/scan the calculated intensity of a single scan for a rotor packed with 40 mg of sample and after full magnetization build-up and $[S/N]_{norm}$/scan is defined analogously. Uncertainties are estimated from noise standard deviation after apodization.

$x_{Fe(III)}$	µW	Mass (mg)	t_1 (s)	signal recovered	ns	t_{tot} (min)	S (a.u.)	S_{norm} /scan (a.u.)	$\varepsilon_{ON/02OFF}$	$\varepsilon_{ON/OFF}$	S/N	$[S/N]_{norm}$ /scan
0.02	OFF	40.0	4.8	0.47	19616	1569	3.34	0.36	1	1	5.4	0.08
	ON		4.8	0.47	1024	81.9	10.72	22.27	62±10	62±10	63	4.19
	ON		41	0.95	128	87.5	2.89	23.80	66±10	66±10	48	4.47
0.01	ON	39.6	345	0.94	16	92.0	1.82	119.81	331±50	256±40	86	22.64
0.005	ON	37.6	500	0.88	16	133.3	2.04	136.52	377±60	282±40	107	28.57
0.0025	ON	40.8	1000	0.63	16	266.7	1.70	171.55	474±70	260±40	87	35.21
0.00125	ON	38.8	1000	0.55	16	266.7	1.10	120.81	334±50	195±30	60	26.45

Table S4. ^{17}O parameter for the DNP measurements, where $x_{Fe(III)}$ is the mole fraction of Fe(III), t_1 the recycle delay, ns the number of scans, t_{tot} the total experimental time, S the total integrated intensity of the spectrum, S_{norm}/scan the calculated intensity of a single scan for a rotor packed with 40 mg of sample and after full magnetization build-up and $[S/N]_{norm}$/scan is defined analogously. Uncertainties are estimated from noise standard deviation after apodization.

4. Polarization enhancement via the Solid Effect

For the following derivations we will consider a two spin ½ system where one of the spins is an electronic and the other a nuclear spin. The spin system is shown schematically in Figure 3 a) of the main document. Diagonalization of the interaction Hamiltonian leads to additional relaxation terms, as described by the group of S. Vega[3,4]. We will (safely) disregard the new terms arising from the nuclear relaxation, however, the new terms from the electronic relaxation are not negligible and will create significant paths for zero- (ZQ) and double-quantum (DQ) relaxation. The longitudinal relaxation matrix in the diagonalized frame is:

$$\hat{R}_1 = \begin{pmatrix} 0 & R_{1e} & R_{1n} & R_{1DQ} \\ R_{1e} & 0 & R_{1ZQ} & R_{1n} \\ R_{1n} & R_{1ZQ} & 0 & R_{1e} \\ R_{1DQ} & R_{1n} & R_{1e} & 0 \end{pmatrix}. \tag{S2}$$

From this we will write the relevant rate equations, which can be interpreted as a transformation into Liouville space. For simplicity we will assume a perfectly sharp pulse, in this case, on-resonance with the DQ transition (completely analogue results can be obtained for irradiation at the ZQ transition). Thus, the only coherences we will excite are the DQ coherences whose transverse relaxation is T_{2DQ}[3].

$$\frac{dp_1}{dt} = -p_1 W_{\uparrow}^{ZQ} + p_4 W_{\downarrow}^{ZQ} - p_1 W_{\uparrow}^{e} + p_3 W_{\downarrow}^{e} - p_1 W_{\uparrow}^{n} + p_2 W_{\downarrow}^{n}, \tag{S3}$$

$$\frac{dp_2}{dt} = -p_2 W_{\uparrow}^{DQ} + p_3 W_{\downarrow}^{DQ} - p_2 W_{\uparrow}^{e} + p_4 W_{\downarrow}^{e} - p_2 W_{\downarrow}^{n} + p_1 W_{\uparrow}^{n} + c_{23}\frac{\omega_1}{2} - c_{32}\frac{\omega_1}{2},$$

$$\frac{dp_3}{dt} = -p_3 W_{\downarrow}^{DQ} + p_2 W_{\uparrow}^{DQ} - p_3 W_{\downarrow}^{e} + p_1 W_{\uparrow}^{e} - p_3 W_{\uparrow}^{n} + p_4 W_{\downarrow}^{n} + c_{32}\frac{\omega_1}{2} - c_{23}\frac{\omega_1}{2},$$

$$\frac{dp_4}{dt} = -p_4 W_{\downarrow}^{ZQ} + p_1 W_{\uparrow}^{ZQ} - p_4 W_{\downarrow}^{e} + p_2 W_{\uparrow}^{e} - p_4 W_{\downarrow}^{n} + p_3 W_{\uparrow}^{n},$$

$$\frac{dc_{32}}{dt} = p_3\frac{\omega_1}{2} - p_2\frac{\omega_1}{2} - c_{32}R_{2DQ},$$

$$\frac{dc_{23}}{dt} = -p_3\frac{\omega_1}{2} + p_2\frac{\omega_1}{2} - c_{23}R_{2DQ}.$$

The nuclear polarization at the steady-state arises as a consequence of saturating the DQ transition. Therefore, we will have to compute the population difference between the states connected via the DQ transition, p_2 and p_3.

$$\frac{d(p_2 - p_3)}{dt} = -2p_2W_{\uparrow}^{DQ} + 2p_3W_{\downarrow}^{DQ} - (p_2 + p_1)W_{\uparrow}^{e} + (p_3 + p_4)W_{\downarrow}^{e} \tag{S4}$$
$$- (p_2 + p_4)W_{\downarrow}^{n} + (p_3 + p_1)W_{\uparrow}^{n} + \omega_1(c_{23} - c_{32}).$$

Next we will write the equation entirely in terms of the populations p_2 and p_3. At the steady state condition $\frac{dp_4}{dt} = \frac{dp_1}{dt} = 0$ and combining the rate equations for p_1 and p_4 we obtain after some rearrangements:

$$-(p_2 + p_1)W_{\uparrow}^{e} + (p_3 + p_4)W_{\downarrow}^{e} \tag{S5}$$
$$= -2p_4W_{\downarrow}^{ZQ} + 2p_1W_{\uparrow}^{ZQ} - (p_4+p_2)W_{\downarrow}^{n} + (p_3 + p_1)W_{\uparrow}^{n}.$$

Inserting this into equation (S4) gives:

$$\frac{d(p_2 - p_3)}{dt} = -2p_2W_{\uparrow}^{DQ} + 2p_3W_{\downarrow}^{DQ} - 2p_4W_{\downarrow}^{ZQ} + 2p_1W_{\uparrow}^{ZQ} - 2(p_2 + p_4)W_{\downarrow}^{n} \tag{S6}$$
$$+ 2(p_3 + p_1)W_{\uparrow}^{n} + \omega_1(c_{23} - c_{32}).$$

So far no approximations have been done. For further simplifying this equation some approximations will be necessary, before we proceed to that let us write the transverse magnetization in a convenient way:

$$\frac{d(c_{32} - c_{23})}{dt} = p_3\omega_3 - p_2\omega_1 + \frac{c_{23} - c_{32}}{T_{2DQ}}. \tag{S7}$$

Approximations

First we will assume that the electronic relaxation rate is much faster than any other rate, consequently, the rates between the populations $p_4 = \varepsilon_e p_2$ and $p_1 = \frac{p_3}{\varepsilon_e}$ are constant. Next,

we will asume that $W_{\downarrow}^{ZQ} = \frac{W_{\uparrow}^{DQ}}{\varepsilon_e}$ and $W_{\uparrow}^{ZQ} = \varepsilon_e W_{\downarrow}^{DQ}$. This means that the ZQ and DQ relaxation rates are equal. Both these approximations only require that the population difference due to the energy difference of the electrons is much larger than due to the nuclei, $(1-\varepsilon_e) \gg (1-\varepsilon_n)$, which of course is always the case in the high temperature approximation.

Inserting these approximations into the terms affected by the ZQ and DQ relaxation rates in equation (S6) leads to:

$$\frac{d(p_2-p_3)}{dt} = -2(2p_2W_{\uparrow}^{DQ} - 2p_3W_{\downarrow}^{DQ}) - 2(p_2+p_4)W_{\downarrow}^{n} + 2(p_3+p_1)W_{\uparrow}^{n} + \omega_1(c_{23}-c_{32}). \tag{S8}$$

In analogy to the single spin ½ system[5] we will introduce the variables $N = p_2 + p_3$ and $n = p_2 - p_3$.

$$\frac{d(p_2-p_3)}{dt} = 2\left(N\left(W_{\downarrow}^{DQ} - W_{\uparrow}^{DQ}\right) - n\left(W_{\downarrow}^{DQ} + W_{\uparrow}^{DQ}\right)\right) - 2(p_2+p_4)W_{\downarrow}^{n} + 2(p_3+p_1)W_{\uparrow}^{n} + \omega_1(c_{23}-c_{32}), \tag{S9}$$

and

$$\frac{d(p_2-p_3)}{dt} = 2\frac{(n_0-n)}{T_{1DQ}} - 2(p_2+p_4)W_{\downarrow}^{n} + 2(p_3+p_1)W_{\uparrow}^{n} + \omega_1(c_{23}-c_{32}). \tag{S10}$$

In the last step we used: $n_0 = (p_2-p_3)_{eq} = N\frac{\left(W_{\downarrow}^{DQ} - W_{\uparrow}^{DQ}\right)}{\left(W_{\uparrow}^{DQ} + W_{\downarrow}^{DQ}\right)} = N\frac{1-\varepsilon_e}{1+\varepsilon_e}$ and $W_{\uparrow}^{DQ} + W_{\downarrow}^{DQ} = \frac{1}{T_{1DQ}}$. In agreement with the definitions given by Hovav et al.[3].

Next we will focus on the terms affected by the nuclear relaxation rate, therefore, we use again the relations $p_4 = \varepsilon_e p_2$ and $p_1 = \frac{p_3}{\varepsilon_e}$:

$$-2(p_2 + p_4)W_{\downarrow}^n + 2(p_3 + p_1)W_{\uparrow}^n = -2p_2 W_{\downarrow}^n(1 + \varepsilon_e) + 2p_3 W_{\uparrow}^n\left(1 + \frac{1}{\varepsilon_e}\right) \tag{S11}$$

$$= N\left(-W_{\downarrow}^n + W_{\uparrow}^n - W_{\downarrow}^n\varepsilon_e + \frac{W_{\uparrow}^n}{\varepsilon_e}\right) + n\left(-W_{\downarrow}^n - W_{\uparrow}^n - \frac{W_{\uparrow}^n}{\varepsilon_e} - W_{\uparrow}^n\varepsilon_e\right)$$

$$= N\left(\frac{W^n}{\varepsilon_e} - W^n\varepsilon_e\right) - n\left(2W^n + W^n\left(\frac{1}{\varepsilon_e} + \varepsilon_e\right)\right)$$

$$= N\left(W^n\left(\frac{1}{\varepsilon_e} - \varepsilon_e\right)\right) - 2n(2W^n).$$

Where we made use of the fact that $(1 - \varepsilon_e) \gg (1 - \varepsilon_n)$ and therefore, $W_{\downarrow}^n \approx W_{\uparrow}^n$, relative to the other rates. And in the last step we assumed that $\varepsilon_e \approx 1$ and therefore $\frac{1}{\varepsilon_e} + \varepsilon_e \approx 2$ which is valid for high temperatures. This expression can be further simplified:

$$N\left(W^n\left(\frac{1}{\varepsilon_e} - \varepsilon_e\right)\right) - 2n(2W^n) = N\frac{\left(W^n\left(\frac{1}{\varepsilon_e} - \varepsilon_e\right)\right)}{(2W^n)}(2W^n) - 2n(2W^n) \tag{S12}$$

$$= N\left(\frac{\left(\frac{1}{\varepsilon_e} - \varepsilon_e\right)}{2}\right)R_{1n} - 2nR_{1n}$$

$$= 2\frac{(n_0 - n)}{T_{1n}}$$

With $2W^n = \frac{1}{T_{1n}}$. In the last step we made the following approximation: $\left(\frac{1}{\varepsilon_e} - \varepsilon_e\right) \approx 4\frac{1-\varepsilon_e}{1+\varepsilon_e}$. Which can be shown to be true for $\varepsilon_e \to 1$, and is good approximation at 100 K and 9.4 T, where $\varepsilon_e \approx 1.135$.

Introducing this result into the derivation of the population difference we get:

$$\frac{d(p_2 - p_3)}{dt} = 2\frac{(n_0 - n)}{T_{1DQ}} + 2\frac{(n_0 - n)}{T_{1n}} + \omega_1(c_{23} - c_{32}) \tag{S13}$$

Finally, at the steady state condition the difference of the population and coherences is constant and we can write:

$$p_2 - p_3 = \frac{(p_2 - p_3)_{eq}}{1 + {\omega_1}^2 T_{2DQ}\left[1/\left(2R_{1DQ} + 2R_{1n}\right)\right]} \tag{S14}$$

References

(1) Harchol, A.; Reuveni, G.; Ri, V.; Thomas, B.; Carmieli, R.; Herber, R. H.; Kim, C.; Leskes, M. Endogenous Dynamic Nuclear Polarization for Sensitivity Enhancement in Solid-State NMR of Electrode Materials. *J. Phys. Chem. C* **2020**, *124* (13), 7082–7090. https://doi.org/10.1021/acs.jpcc.0c00858.

(2) Tse, D.; Hartmann, S. R. Nuclear Spin-Lattice Relaxation Via Paramagnetic Centers Without Spin Diffusion. *Phys. Rev. Lett.* **1968**, *21* (8), 511–514. https://doi.org/10.1103/PhysRevLett.21.511.

(3) Hovav, Y.; Feintuch, A.; Vega, S. Theoretical Aspects of Dynamic Nuclear Polarization in the Solid State – The Solid Effect. *J. Magn. Reson.* **2010**, *207* (2), 176–189. https://doi.org/10.1016/j.jmr.2010.10.016.

(4) Kundu, K.; Mentink-Vigier, F.; Feintuch, A.; Vega, S. DNP Mechanism. In *eMagRes*; WILEY-VCH Verlag GmbH & Co. KGaA, 2019; Vol. 8, pp 295–338. https://doi.org/10.1002/9780470034590.emrstm1550.

(5) Slichter, C. P. *Principles of Magnetic Resonance*, 1st ed.; Harper & Row: New York, 1963.